Motion Noise Cancelation in Heartbeat Sensing using Accelerometer and Adaptive Filter

Shahab Ardalan, *Senior Member, IEEE*, Siavash Moghadami, *Graduate Student Member, IEEE*, and Samira Jaafari

***Abstract*—This letter focuses on suppressing the motion artifact of wrist photoplethysmographic heart rate signals using an accelerometer based adaptive filter. Monitoring of the heart signal can offer important insights with regard to health and wellness. The objective of the experiment conducted here is to recover the distorted signal resulting from body movement while measuring the heart rate signal noninvasively from the wrist. The class of filters, known as adaptive filters, that can extract meaningful information from the distorted signal, used predetermined initial conditions to equalize the signal distortion due to motion. Adaptive filters of least mean-square (LMS), Kalman filter, and recursive least-squares (RLS) were used in this study to recover the distorted heart rate signal. This study also presented a comparison on utilized filters that can be used for recovering of the heart rate signal.**

***Index Terms*—Body sensors, health, heart rate signal, photoplethysmography, vital signs, wearable.**

I. Introduction

THE heart rate signal is one of various biomedical signals transmitted throughout the human body. Monitoring this signal leads to important information about the state of this critical organ, with important implications for an individual's health [1].

Noninvasive heart rate monitors have been integrated into wristwatches and fitness machines that display caloric expenditure during exercise and body movement [2]. Fitness machines have metal sensors that, only when in contact with both palms simultaneously, are able to detect and display the heart rate. However, holding on to metal sensors without interruption during exercise can be problematic in the context of high intensity movement. Chest strap sensors represent an alternative for overcoming this problem, as they remain in contact with the body even during the most intensive exercise.

Devices that can accurately measure the hemoglobin oxygen saturation content together with the heart rate are known as pulse oximeters [3]. Pulse oximetry refers to the noninvasive measurement of the level of oxygen saturation and of the pulse rate in veins. Pulse oximeters are generally used in the medical field for taking a variety of body measurements. Blood circulates throughout the body in rhythm with the heartbeat [4]. Thus, measuring the signal of the rate that blood moves throughout the body is one way of gauging the heart rate [5].

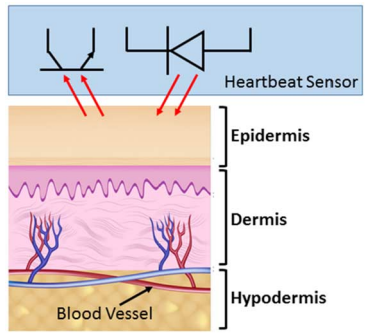

Fig. 1. The principle of heartbeat sensor.

A noninvasive optical method of measuring the heart rate with the use of light-emitting diodes (LEDs) and photodiodes is known as photoplethysmography [6]. Using this technique, as clearly shown in Fig. 1, light directed toward the skin is partially absorbed by hemoglobin, with the remainder of the light reflected off of the skin or anatomical layers beneath the skin, as blood pulsates throughout the veins [7].

With photoplethysmography, heart rate can be gauged by measuring the amount of reflected light. Although the backscattered light is not in sync with the heart beat when the body is in motion, the signal can be recovered using various adaptive filters [8]. Although, the adaptive filters may not be able to recover the signal perfectly as the body motion can be changed randomly and abruptly. Therefore, in the proposed technique, an accelerometer has been used to collect the body motion information. This information is used by adaptive filters to recover the heartbeat more accurately.

II. Adaptive Filters

Various types of interference distort the heart rate signal during photoplethysmographic (PPG) monitoring as a result of body movement [1]. Intersymbol interference (ISI) that distorts the signal is caused by light absorption in the skin, tissues, and muscles. Light absorption reduces the amount of backscattered light at the receiving end, as well as the peak-to-peak amplitude of the signal.

The heart rate signal is measured by the circulation of blood in veins during body movement. Specifically, the amount of light that is reflected back to the photodiode is directly proportional to the frequency at which the heart pumps blood throughout the body. The amplitude of the signal, based on the amount of

Manuscript received February 18, 2015; revised May 27, 2015; accepted July 15, 2015. Date of publication July 17, 2015; date of current version December 01, 2015. This manuscript was recommended for publication by M. Balakrishnan.

The authors are with the Center for Analog and Mixed-Signal, Department of Electrical Engineering, San Jose State University, San Jose, CA 95192 USA (e-mail: ardalan@ieee.org; siavash.moghadami@sjsu.edu; samjaafari@yahoo.com).

Color versions of one or more of the figures in this letter are available online at http://ieeexplore.ieee.org.

Digital Object Identifier 10.1109/LES.2015.2457933

backscattered light measured by the photodiode, increases or decreases at the same frequency that blood is pumped by the heart. The properties of the resulting signal can aid in digital processing and assist in gauging a reliable heart rate. Many types of filters are prevalent in signal processing. Filters manipulate signals to reject unwanted characteristics. Noise, interferences, and erroneous frequencies are undesirable characteristics that affect data in signals. These unwanted attributes can be extensively minimized or nearly eliminated with the use of filters. An adaptive filter, also known as a transversal filter, is one that self-adjusts its parameters to converge to specified target values. Adaptive filters are useful when the characteristics of the incoming signal are unknown or likely to vary.

An adaptive filter uses a recursive algorithm to adjust its parameters based on predetermined initial conditions. The filter output converges to target values after several parameter iterations. Choosing which recursive algorithm to implement is determined by the prioritization of the following adaptive filter characteristics: rate of convergence, misadjustment, tracking, robustness, computational requirements, structure, and numerical properties [9].

Three types of adaptive filters, LMS, RLS, and Kalman were used on the same data sets to compare their performances. The incoming data to the PPG sensor were supplemented with a separate reference input from an accelerometer that was also located next to the PPG sensor. ADXL335 was used as a triple-axis accelerometer with INTEL Galileo Gen 1. The PPG sensor, which is an open-source sensor, and the accelerometer were linked to the INTEL Galileo Gen 1 that was connected to a computer for data transfer and storage.

The LMS algorithm has low computational complexity and functions as a widely used algorithm for FIR adaptive filters [10]. The algorithm is a member of the family of stochastic gradient algorithms and produces the least mean-square of the error signal [9]. The RLS algorithm recursively derives the filter coefficients that minimize a weighted least-squares cost function, known as error signal, in an adaptive filter. Unlike the LMS, the RLS belongs to the class of deterministic input signals and has a rate of convergence that is typically an order of magnitude faster [9]. However, the high convergence rate consists of high computational complexity. Theoretically, the Kalman filter is also a recursive system for noise cancelation. The filter allows exact inference in a linear dynamical system, which is a Bayesian model. The Kalman filter uses control inputs to that system, and multiple sequential measurements to form an estimate of the system's varying quantities [11].

III. System Description

Fig. 2 shows the entire topology of the system along with a sensor for INTEL Galileo Gen 1 that the heart rate signal was measured with, known as the PPG pulse sensor [see Fig. 2(b)] and the accelerometer. The reference input to the adaptive filter was the accelerometer signal. Fig. 2(c) pictures the front of the accelerometer and the direction of each axis. Both of the signals were inputs to the microcontroller that applied LMS, RMS and Kalman filters then transmitted data to a computer. The microcontroller board was an INTEL Galileo Gen 1 with an Intel Quark SoC X1000 processor, depicted in Fig. 2(a).

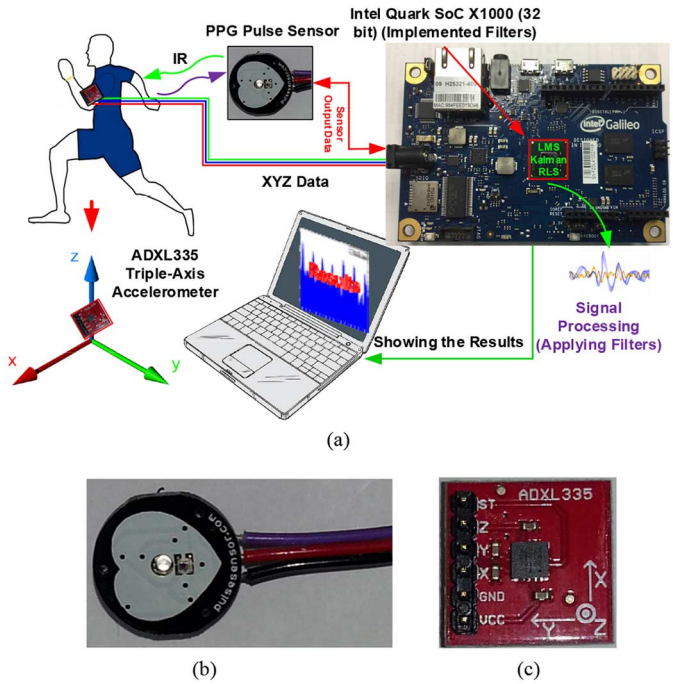

Fig. 2. (a) Topology of the accelerometer-based heartbeat sensor. (b) PPG Pulse Sensor (c) ADXL335 triple-axis accelerometer.

The PPG sensor and accelerometer signals were wired to the microcontroller analog inputs. The four signals were passed through ADCs that quantized the voltage levels to digital values in the range of 0 to 1024. The filters has been implemented using INTEL Galileo Gen 1 where it samples the heart rate and the accelerometer signals at 125 Hz, or every 16 ms. The signals were in the frequency range of 0.66 to 3.3 Hz. Thus, the sampling rate obeyed the Nyquist criterion. The transmitted data to the INTEL Galileo Gen 1 serial monitor and saved in a text file for further processing. Processing the signals required importing the recorded data from the text file into the MATLAB workspace.

IV. Experimental Results

It is important to note the condition of the heart rate signal before processing the distorted signal. The heart rate signal, illustrated in Fig. 3, clearly shows the peaks of each pulse in a six-second window. Seven noticeable pulses were recorded when there was no body movement. The INTEL Galileo Gen 1 controlled the PPG sensor to maintain a mean voltage of $V_{DD}/2$, where V_{DD} was 3.3 V. The ADC midpoint value was 512 and each peak above that value corresponded to one heart pulse. The heart rate signal was distorted during body movement. The anatomy of the wrist also affected the signal integrity during body movement. The reconstruction of the heart rate signal was possible with the implementation of adaptive filters. The adaptive filters were applied to the distorted signal in Intel Quark SoC X1000 for signal reconstruction. The heart rate signal was recorded for roughly 45 s during four distinct periods of time. The four distinct periods include no body movement, movement in each axial direction alone, and are roughly 10 s each. The heart rate and accelerometer signals are illustrated in Fig. 4, to show their relationship in each window of time. The heart rate signal was distorted during body movement in the three axial

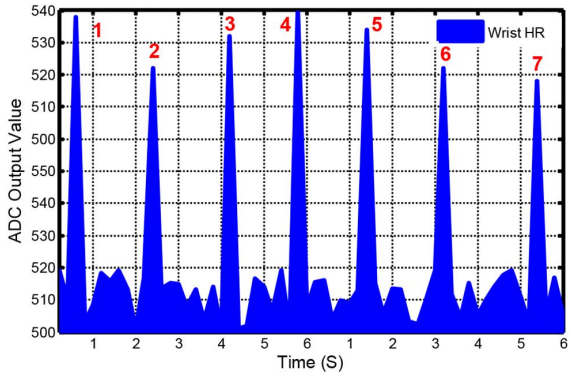

Fig. 3. Resting wrist PPG heart pulse clearly shows seven pulses in six seconds (after threshold filter).

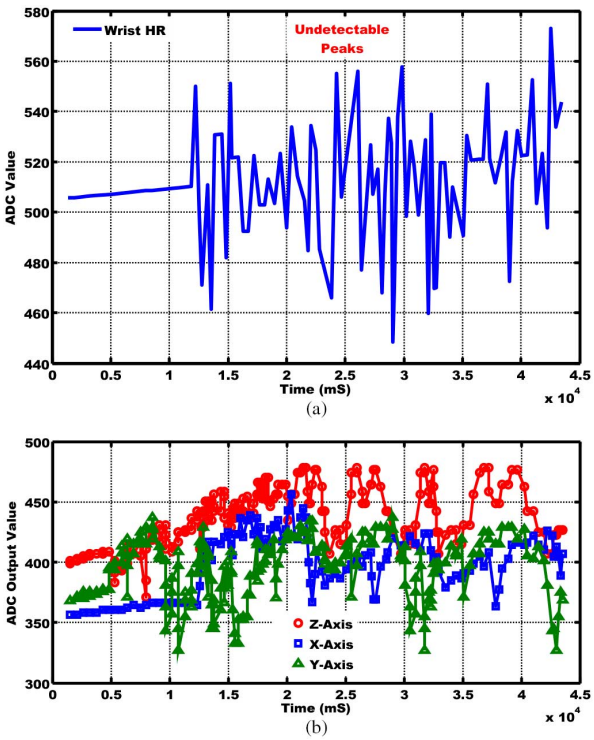

Fig. 4. (a) During body movement, the heart rate signal from the PPG sensor becomes distorted. (b) Accelerometer X, Y, Z signals are the supplemental input to the adaptive filters for signal recovery.

directions in comparison to the period of no body movement. It is important to note that the signals were superposed on the same plot and reduced to unit amplitude for signal processing.

The LMS adaptive filter was applied to nine sets of data to produce nine unique system outputs. The nine sets correspond to the X, Y, and Z axes in the last three time periods, illustrated in Fig. 4.

A. LMS Adaptive Filter

The adaptive filter was tested on different step-sizes μ and filter lengths M, with only one parameter changed per test. The step-size μ and the filter length M influenced the filter coefficients or tap weights.

Various step-sizes were used to compare the system outputs. The smaller the step-size was, the more time it took for the output to converge. Conversely, the larger the step-size was, the greater the jump was in the system output. A series of tests can provide a reasonable value for the step-size. Nonetheless, it is favorable to have a slower convergence rate and a more accurate output than a fluctuating and a noisy output due to a large step-size value. Fig. 5(a) illustrates the result of applying LMS filter with M and step-size of 100 and 0.008, respectively.

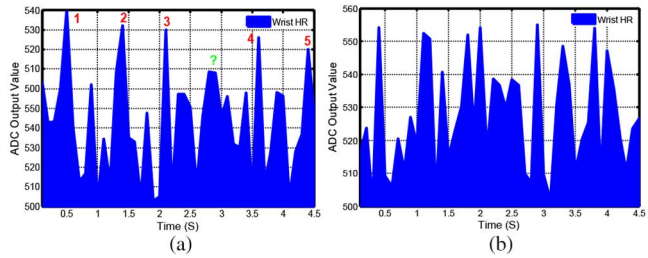

Fig. 5. Filtered heartbeat signal (ADC output). (a) LMS. (b) RLS.

The filter order length is another critical factor in the performance of the adaptive filter. Filter order lengths of 10 and 100 with the same step-sizes were tested to compare differences in the system output. The greater the filter length was, the more complex the computations were.

The correlation for the X and Y accelerometer signals with the heart rate signal for movement in the Y direction appeared to be higher than any of the same signals with movement in the X direction. The filter output for heart rate signal with movement in the XYZ directions is shown in Fig. 5(a) where the filter order is 100 and step size of 0.008. The intended system output results should closely resemble the characteristics of the resting heart rate in Fig. 3, where the peaks of the heart pulse are distinct.

There was a clear time lag between the accelerometer signals and the heart rate signal. Intuitively, this lag implied that there was a change in the heart rate after some movement had occurred. Nonetheless, the system output of the LMS adaptive filter in Fig. 5(a) partially recovered the heart rate signal with the aid of the accelerometer signals. The same sets of the data were passed through RLS adaptive filters and compared to the system outputs of the LMS adaptive filters.

B. RLS Adaptive Filter

The RLS adaptive filter is computationally more complex than the LMS adaptive filter. However, the tradeoff for the increased complexity is the improved accuracy. The data sets were used on the LMS adaptive filter were also used on the RLS adaptive filter for more accurate comparison between the two filter types.

The parameters for the RLS adaptive filter included the filter order length, the forgetting factor, and the inverse covariance matrix. When the forgetting factor λ is zero, the RLS adaptive filter has no memory. Conversely, when the forgetting factor λ is one, the RLS adaptive filter has an infinite memory. This means that the current value that is being processed by the adaptive filter contains information on the previous output values from the very instant the algorithm starts processing the data. It is important to note that infinite memory is very difficult to implement in reality and a λ value close to one, but not equal to one, is more realistic.

The system output was very noisy with a forgetting factor of 0.09 and a filter order length of 10, illustrated in Fig. 5(b). The filter outputs for the accelerometer X-axis are shown in Fig. 5(b). The top plot corresponds to the input that was passed to the RLS adaptive filter and the bottom plot corresponds to the system output of the filter. The data in the top plot is taken from the second time period in Fig. 4 with movement in the X direction. The noisy output implied that the lack of memory of the previous output values caused large overcompensations in the current value that was being processed by the adaptive filter. The small values of lambda perform poorly due to the inherent recursive property of the RLS algorithm.

The data sets with movement in the Y direction provided the best results, similar to the LMS adaptive filter results. The high correlation between the primary and reference inputs allowed the filter outputs to recover the heart rate signal partially. The remaining data sets might have had the capabilities of reconstruction had inputs been more closely correlated with each other.

C. Kalman Adaptive Filter

In order to reconstruction the distorted heartbeat signal, Kalman Filter (KF) arrangement is used to minimize the variance of the error (e) between the measured output (y_k) and the estimated output y'_k

$$e(k) = y(k) - y'(k) = y(k) - C_k X_k. \quad (1)$$

Where C is the vector of measurement history and X is the vector of unknown parameters. Regarding [12], in order to cancel the effects of artifacts, it can be written that

$$X_{k+1} = AX_k \quad (2)$$

$$P_k = (A - K_k C_k)\, P_k (A - K_k C_k)^T + \varepsilon K_k K_k^T. \quad (3)$$

Where K is Kalman gain and P is uncertainty matrix and ε is a positive value less than one. The convergence time for the KF approach depends on the initial value of P. The filter convergence time and delay is a key factor for this application. Therefore, the initial value has been select as 20 times of the identity matrix. Fig. 6 shows the filtered data and reconstructed heart rate.

V. Summary and Conclusion

Several various attempts have been done to reduce or nearly eliminate the drawbacks of motion artifacts in heartbeat sensors. A simple heartbeat detection approach using heart-beat rate variability (HRV) is applied in [13]. However, the overall system performance is limited to the fast motion artifact since there is a time interval of 10 second between the detected artifacts. The comprehensive PPG study is reported in [14] utilizing LMS and RLS adaptive filters to cancel the noises arise from motion artifacts. It is shown that although both RLS and LMS adaptive filters cannot fully detect and eliminate the motion artifacts which I could be seen in presented experimental result well. Furthermore in [15], a complex 4th order normalized least mean square (NLMS) adaptive filter is used to reduce the motion artifacts for just two-dimensions (x-y). Their results demonstrated the necessity of having a three-dimensional motion artifact cancellation system. In this letter, an efficient usage of

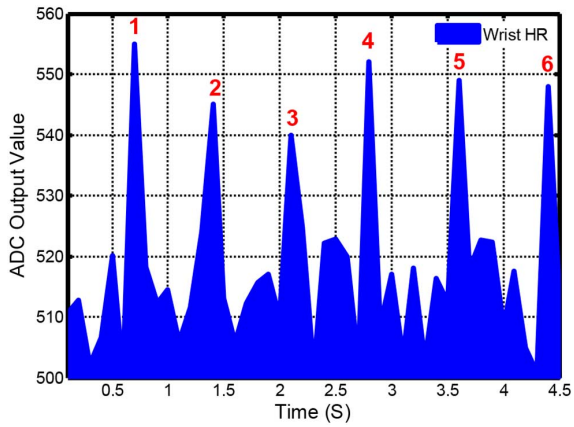

Fig. 6. Kalman Filter results for the heart rate signal.

Kalman adaptive filter (implemented in INTEL Galileo Board) is reported with promising results to cancel the drawbacks of motion artifacts in three dimensions. The filtered data precisely predicted the heart rate.

References

[1] P. T. Gibbs, L. B. Wood, and H. H. Asada, "Active motion artifact cancellation for wearable health monitoring sensors using collocated MEMS accelerometers," *Int. Soc. Opt. Eng.*, pp. 811–819, May 2005.

[2] Y. K. Lee, J. Jo, and H. S. Shin, "Development and evaluation of a wristwatch-type photoplethysmography array sensor module," *IEEE Sensors J.*, vol. 13, no. 5, pp. 459–1463, May 2013.

[3] M. Izzetoglu, A. Devaraj, S. Bunce, and B. Onaral, "Motion artifact cancellation in NIR spectroscopy using wiener filtering," *IEEE Trans. Biomed. Eng.*, vol. 52, no. 5, pp. 934–938, May 2005.

[4] W. Kist, "Comparison of two pulse oximeters during sub-maximal exercise in healthy volunteers: Effects of motion," *J. Exercise Physiol.*, vol. 5, no. 1, pp. 42–48, Feb. 2002.

[5] J. E. Hall, *Guyton and Hall Textbook of Medical Physiology*. Philadelphia, PA, USA: Saunders Elsevier, 2011, p. 107.

[6] R. Dresher, "Wearable Forehead Pulse Oximetry: Minimization of Motion and Pressure Artifacts," master's thesis, Worcester Polytech. Inst., Worcester, MA, USA, 2006.

[7] L. J. Mengelkoch, D. Martin, and J. Lawler, "A review of the principles of pulse oximetry and accuracy of pulse oximeter estimates during exercise," *J. Amer. Phys. Therapy Assoc.*, vol. 74, no. 1, pp. 40–49, Jan. 1994.

[8] T. Tamura, Y. Maeda, M. Sekine, and M. Yoshida, "Wearable photolethysmographic sensors-past and present," *Electronics*, Apr. 2014.

[9] S. Haykin, *Adaptive Filter Theory*, 4th Ed. ed. Englewood Cliffs, NJ, USA: Prentice Hall Inc., 2002.

[10] A. D. Poularikas and Z. M. Ramadan, *Adaptive Filtering Primer with MATLAB*. Boca Raton, FL, USA: CRC Press, 2006.

[11] R. Faragher, "Understanding the basis of the kalman filter via a simple and intuitive derivation," *IEEE Signal Process. Mag.*, vol. 29, no. 5, pp. 128–132, Sep. 2012.

[12] B. Widrow, J. M. M. Michael, G. Larimore, and C. Richard Johnson, "Adaptive noise canceling: Principles and applications," *Proc. IEEE*, vol. 163, no. 12, pp. 1692–1716, Dec. 1975.

[13] S. Arberet, M. Lemay, P. Lenevey, J. Sola, O. Grossenbacher, D. Andries, C. Sartouri, and M. Bertschi, "Photoplethysmography-based ambulatory heartbeat monitoring embedded," in *Proc. Comput. Cardiol. Conf. (CinC)*, Sep. 2013, pp. 935–938.

[14] H. Han, M. J. Kim, and J. Kim, "Development of real-time motion artifact reduction algorithm for a wearable photoplethysmography," in *Proc. 29th Annu. Int. Conf. Eng. Med. Biol. Soc. (EMBS)*, Aug. 2007, pp. 1538–1541.

[15] C. Dickson, "Heart Rate Artifact Suppression," master's thesis, Grand Valley State Univ., Allendale, MI, USA, 2012.

[16] W.-K. Chen, *Linear Networks and Systems*. Belmont, CA, USA: Wadsworth, 1993, pp. 123–135.